

MODERN APPROACHES TO OBTAINING CONTINUOUS COOLING TRANSFORMATION DIAGRAMS FOR WELDING (REVIEW)

V.V. Zhukov, V.A. Kostin, S.G. Hrygorenko, R.S. Gubatyuk

E.O. Paton Electric Welding Institute of the NASU
11 Kazymyr Malevych Str., 03150, Kyiv, Ukraine

ABSTRACT

The article presents a review of modern approaches to constructing CCT diagrams and special diagrams formed on the basis of the results of a dilatometric experiment for the analysis of structural-phase transformations in steels during cooling. The methodology of physical modeling of thermal cycles on Gleeble installations, as well as typical heating and cooling parameters, is considered. Special attention is paid to the influence of the cooling rate on the formation of the microstructure in the heat-affected zone of welded joints. Approaches using constant and variable (nonlinear) cooling modes are compared with an emphasis on their compliance with real welding conditions. The advantages of nonlinear thermal cycles for increasing the reliability of modeling and correctness of constructing CCT diagrams when assessing the weldability of steels are substantiated.

KEYWORDS: physical modeling, phase transformations, microstructure, austenite, martensite, CCT and DCCT diagrams, Gleeble, welded joints

INTRODUCTION

Continuous cooling transformation (CCT) diagrams of overcooled austenite decomposition are an important tool for analysis of the structural-phase transformations in steels during cooling. They reflect how the austenite structure changes at different cooling rates, i.e. how the phase (ferrite, pearlite, bainite or martensite) is formed, depending on the temperature and time [1–3].

Using the CCT diagrams specialists can:

- Predict the structure in each HAZ — know whether martensite (leading to brittleness) or ferrite/pearlite (ensuring the ductility) are formed;
- Assess the risk of cold cracking, which is often associated with appearance of martensite at rapid cooling;
- Select the welding modes (current, welding speed, preheating/additional heating), so as to reduce the harmful structural changes;
- Determine the need for postweld heat treatment.

Thus, CCT diagrams are extremely important in welding critical structures — from pipelines to armour, where control of the metal structure and properties in the HAZ is required.

A dilatometric experiment is the base of experimental plotting of CCT diagrams. This is a method of studying phase transformations in materials based on measurement of changes in the linear dimensions of the sample during the thermal cycle (heating or cooling). It is conducted using a dilatometer — a high-precision instrument, which records the material deformation with micron accuracy at temperature change.

A steel sample is heated up to austenitization temperature (above A_{c3}), and held for a certain time for structure stabilization. Then, the sample is cooled down at a constant specified rate (for instance, 1 °C/s). During cooling, the dilatometer records the change in sample length in real time. In the phase transformation points (austenite-ferrite, pearlite, bainite, etc.) jump-like or characteristic changes of the deformation curve occur, which are recorded by the instrument [4]. In Ukraine, unfortunately, there is still no standard which specifies the CCT diagram construction, as well as conducting the dilatometric experiment.

ASTM A1033-18 (2023) Standard [5] entitled “Standard Practice for Quantitative Measurement and Reporting of Hypoeutectoid Carbon and Low-Alloy Steel Phase Transformations”, describes a procedure for quantitative measurement and presentation of phase transformations in hypoeutectoid carbon and low-alloy steels, using high-speed dilatometry. In Section 1.3 of this Standard it is noted that the procedure is used to determine the behaviour of phase transformations in steels, both under the isothermal conditions and under the conditions of continuous cooling. Although the CCT diagram term is not used directly, the described methods allow obtaining data, required to plot such diagrams. Thus, the Standard does not contain any direct reference to CCT diagrams, but provides a methodology, which allows obtaining information for their construction.

In ASTM A1033-18 Standard (2023) the procedure for plotting these phase transformations envisages using linear (i.e. constant) cooling rates. If it is impossible to control the constant rate, (for instance,

in the real technological process), it is necessary to record the instantaneous cooling rate at 700 °C and cooling duration in the range of 800–500 °C.

THE OBJECTIVE OF THE WORK

is to analyze the modern methods of construction of CCT diagrams of phase transformations under the conditions of welding, with the purpose of taking into account the complex temperature-mechanical influences and the nonlinear nature of the thermal cycle of welding.

Quite often the CCT diagrams, plotted with application of constant cooling rates, are used to assess the structural-phase composition of steels in the HAZ. For instance, in [6] the microstructural transformations in the HAZ of pipeline steel X70 (C — 0.06 %; Mn — 1.28 %; Si — 0.26 %; Nb — 0.045 %; Ti — 0.014 %; Mo — 0.17 %) during the thermal cycles of welding were studied. Experiments were conducted in Gleeble 3500 installation. To study the phase transformations, the samples were heated at the rate of 10 °C/s up to the maximal temperature of 1300 °C, then cooled to 900 °C in 1 s, held for 16 s at this temperature, and then cooled to room temperature at constant cooling rates from 60 to 0.1 °C/s. It should be noted that the diagram was plotted at the temperature of 900 °C. The authors conclude that the optimal cooling rate to ensure the HAZ strength and toughness is equal to 10–20 °C/s (Figure 1).

Work [7] presents the construction of a CCT diagram for the HAZ of carbon steel SA106 Grade B (C — 0.3 %; Mn — 0.7 %; Si — 0.1 %; Cr — 0.4 %; Cu — 0.4 %; Mo — 0.15 %; Ni — 0.4 %; V — 0.08 %). The objective of the study was evaluation of the phase transformations and the microstructure, which form in the HAZ at different cooling rates, which reproduces the arc welding conditions.

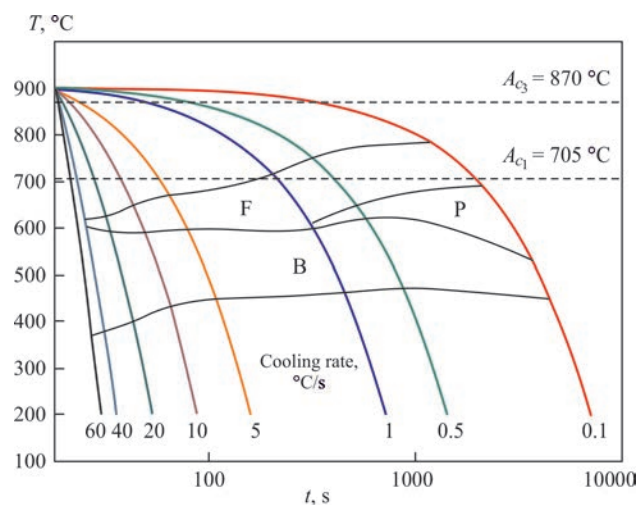


Figure 1. CCT diagram of pipe steel X70. Microstructures: F — ferrite; B — bainite; P — pearlite [6]

The dilatometric experiment was conducted in Gleeble 3500 installation. Samples were heated at the rate of 100 °C/s up to 1200 °C, held at this temperature for 1 s and cooled to room temperature at the specified constant rates from 0.1 to 100 °C/s. The general conclusions indicate that the optimal cooling range to form a favorable structure is 10–20 °C/s. The derived CCT diagram is recommended for development of technologies for welding steel SA106 Grade B (Figure 2).

In work [8] the influence of different cooling rates on the HAZ microstructure was studied and a CCT-diagram was constructed for the conditions of welding CLAM steel (China Low Activation Martensitic, C — 0.093 %; Cr — 8.39 %; W — 1.499 %; V — 0.196 %; Ta — < 0.01 %; Mn — 0.44 %), which is a ferritic-martensitic steel designed for application in nuclear reactors.

Physical modeling was performed in Gleeble-1500 installation. The thermal cycle included heating up to the temperature of 1623 K (~ 1350 °C) in 2 min, holding for 1 min and cooling to room temperature at constant cooling rates in the range of 3600–1 K/min (60–0.017 °C/s). The plotted CCT diagram has only two regions of phase transformations: ferritic and martensitic. The authors note that the diagram allows predicting the HAZ structure, and it is a useful tool to assess the weldability of CLAM steel (Figure 3).

Although the authors present the above-considered works on CCT diagram construction as studies of the HAZ influence on the steel structure in welding, the cooling rate ranges used during CCT diagram construction in these works are very similar to those applied in the works on CCT diagram construction for determination and optimization of the heat treatment cycles.

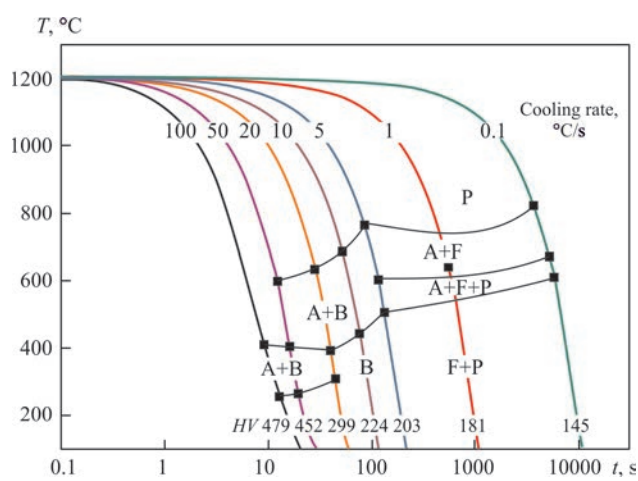


Figure 2. CCT diagram of steel SA106 Grade B. Microstructures: A — austenite; F — ferrite; B — bainite; P — pearlite; M — martensite [7]

In [9] the behaviour during continuous cooling of steel similar to the ferritic-martensitic CLAM steel in [8] was studied. The main objective is construction of CCT diagram and studying the influence of the cooling rate on phase transformation and microhardness. In this work, however, the efforts were focused on development of heat treatment of this steel.

Physical modeling was conducted in Gleeble 1500 installation. The samples were heated to 1253 K ($\approx 980^\circ\text{C}$) in 15 min, held for 30 min, and then cooled to room temperature at the rates from 240 K/min (4°C/s) to 1 K/min (0.017°C/s). All the thermal cooling cycles were conducted at a constant rate. The authors note that the obtained results can be used to develop heat treatment modes with predicted phase composition in the critical zones of nuclear reactor structures (Figure 4).

The conditions of plotting the CCT diagrams differ for each case, and conducting the dilatometric experiment essentially is physical modeling of the technological influence on the material. If during the technological processing of the material, the thermal influence is accompanied by deformational impact, it should be taken into account, when studying the kinetics of the phase-structural transformations.

A description of the so-called DCCT diagrams (Deformation Continuous Cooling Transformation) is sometimes found in publications. Such diagrams are used for optimization of the modes of thermodeformational treatment and they appeared due to the need to allow for the influence of thermodeformational treatment on the kinetics of structural-phase transformations. So, work [10] is a study of the influence of prior plastic deformation on the nature of CCT diagram of spring steel 51CrV4 ($\text{C} - 0.47\text{--}0.55\%$; $\text{Si} - \leq 0.40\%$; $\text{Mn} - 0.70\text{--}1.10\%$; $\text{P} - \leq 0.025\%$; $\text{S} - \leq 0.035\%$; $\text{Cr} - 0.90\text{--}1.20\%$; $\text{V} - 0.10\text{--}0.25\%$).

Both a standard CCT diagram and a DCCT diagram, which allows for the deformation before cooling of 51CrV4 steel (Figure 5) were plotted in Gleeble 3800 simulator.

To construct the CCT diagrams without deformation, the samples were heated to 850°C , held for 120 s and were cooled at constant rates in the range of $0.16\text{--}12^\circ\text{C/s}$. In the cycles with deformation, the samples after similar holding were uniaxially compressed at 850°C with true deformation of 0.35 at the rate of 1 s^{-1} , and then cooled at the same rates. The cooling rate was constant for all the cooling cycles.

DCCT diagram showed a shift of the curve of the start of pearlitic transformation to the left (to the region of higher cooling rates), i.e. pearlite formed faster. The curve of the start of the bainitic transformation somewhat shifted upwards (to higher temperatures),

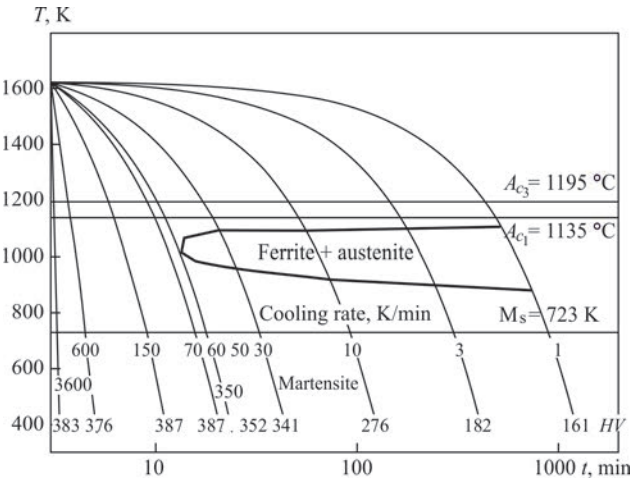


Figure 3. CCT diagram of CLAM steel HAZ [8]

and there appeared also the curve of the end of bainitic transformation. The curve of the start of martensitic transformation has declined a little in the zone of high rates. On the whole, deformation accelerates the anisothermal decomposition of austenite for this steel, which is particularly noticeable for the pearlitic component.

Note that for deformed metal there is a tendency for the transformation acceleration under the conditions of continuous cooling, compared to metal without deformation.

For instance, in [11] the authors studied the influence of chromium content and prior deformation of austenite on the shape of CCT and DCCT diagrams for low-carbon bainitic steels. The objective of the work was to assess how the structure and hardness change, depending on the composition, cooling temperature and deformation. Three steels with the same content of carbon ($\sim 0.033\%$), manganese ($\sim 0.9\text{--}1\%$) and niobium ($\sim 0.06\%$), but with different chromium concentration: 3.97 % (A), 2.52 % (B) and 1.02 % (C) were studied (Figure 6). All the samples were heated up to the temperature of 1100°C at the rate of 10°C/s and were held for 3 min. In order to construct the CCT

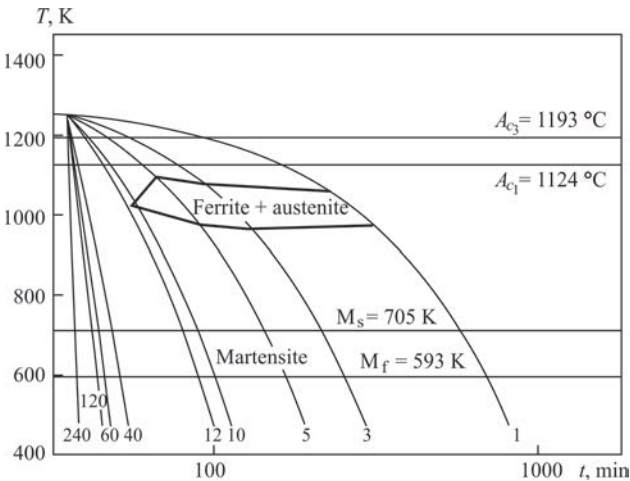


Figure 4. CCT diagram of CLAM steel for heat treatment [9]

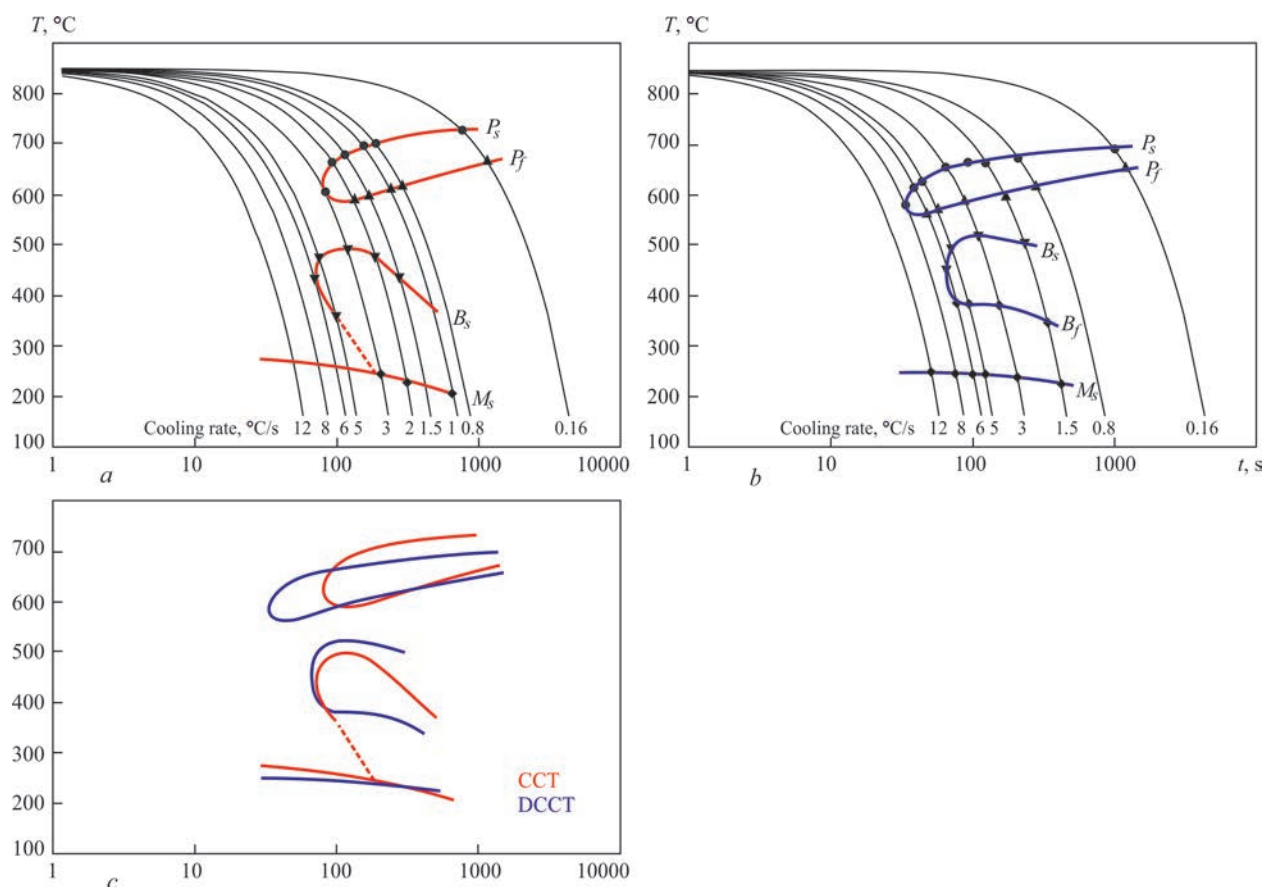


Figure 5. Influence of prior plastic deformation on the kinetics of austenite transformation for 51CrV4 steel: *a* — CCT diagram of steel without deformation; *b* — DCCT diagram of steel with prior deformation; *c* — comparison of CCT and DCCT diagrams. Temperatures: P_s — start of pearlitic transformation; P_f — finish of pearlitic transformation; B_s — start of bainitic transformation; M_s — start of martensitic transformation [10]

diagrams, the samples were cooled to room temperature after holding with different cooling rates, which varied from 2 to 80 °C/s. For plotting the DCCT diagrams, the samples were cooled after holding at the rate of 2 °C/s to the temperature of 880 °C. The samples were held at this temperature for 15 s, and then compressive deformation was applied to them with 0.6 total strain and strain rate of 1 s⁻¹. After deformation, the samples were soaked for another 20 s, and then cooled to room temperature at different cooling rates in the range from 2 to 80 °C/s.

It should be noted that the deformational impact leads to lowering of the temperatures of the start of austenite transformation and to shifting of the ferrite phase appearance towards higher cooling rates (Figure 6). Increase of chromium content improves the hardenability, lowers the phase transformation temperatures, increases the fraction of bainite and reduces the structure sensitivity to deformation. Contrarily, at a low Cr content the deformation stimulates the ferrite formation and essentially changes the transformation kinetics. The authors note that in order to form a completely bainitic structure it is necessary to avoid ferrite and pearlite, which can be achieved at Cr content in

the range of 2.5–4 % and cooling rates above 20 °C/s (Figure 6).

Allowing for deformational impact on the nature of structural-phase transformations is of direct importance in welding. Thermal deformations arising in welding, depending on the structural features of the product being welded, can influence the kinetics of austenite transformation.

For instance, work [12] presents a new approach to analysis of material proneness to developing residual stresses in the welded joint HAZ – so-called “welding thermal stress diagrams” (WTSD). Unlike the classical CCT diagrams, which describe the phase transformations, without taking into account the mechanical limitations, the WTSD diagrams allow directly assessing how the real welding temperature cycles influence the development of stresses in the metal.

Selected for analysis was a high-strength low-alloy steel of ferritic-bainitic class (C — 0.12 %; Si — 0.07 %; Mn — 1.73 %; P — 0.023 %; S — 0.003 %; Al — 0.042 %). The samples were fixed in rigid grips of thermomechanical simulator Gleeble 3550-GTC, which allowed completely blocking the sample elongation during heating and cooling. This ensured development of internal stresses, similar

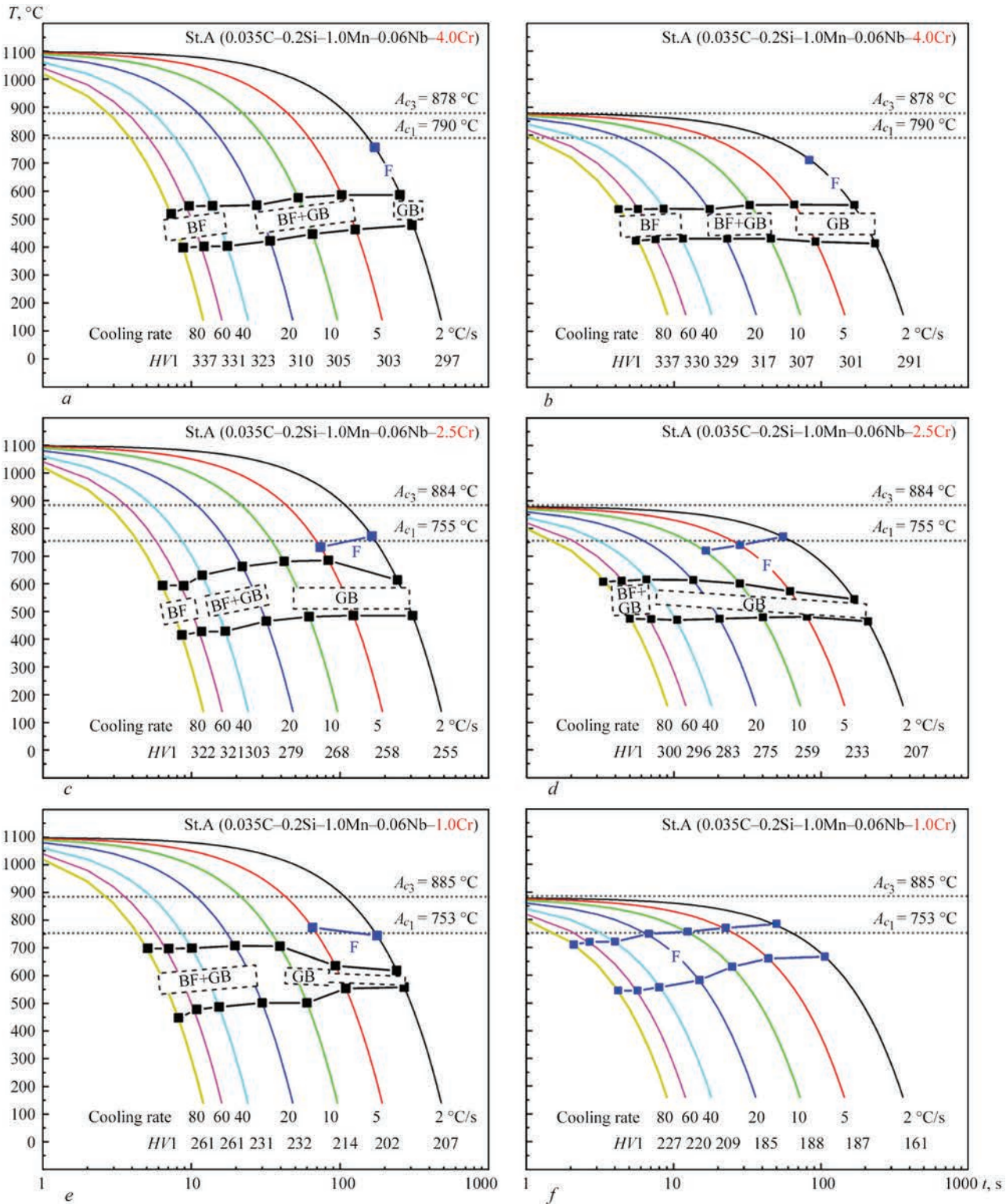


Figure 6. Influence of chromium content and prior plastic deformation on the kinetics of austenite transformation in low-carbon bainitic steels with different chromium content of 3.97 % (A), 2.52 % (B) and 1.02 % (C): *a, c, e* — CCT diagrams; *b, d, f* — DCCT diagrams of steels. Microstructures: BF — bainitic ferrite; GB — granular bainite; F — ferrite [11]

to those formed in the real welded joints. In the work modeling of various HAZ subzones was conducted, which differed by the maximal heating temperature: 1350 °C for coarse-grained HAZ (CGHAZ), 1100 °C for fine-grained HAZ (FGHAZ), 900 °C for intercritical HAZ (ICHAZ) and 700 °C for subcritical HAZ (SCHAZ). After the maximal heating temperature

has been reached, cooling was performed at different cooling rates, equal from 10 to 100 °C/s (in the range of 800–500 °C). It should be noted that for modeling the cooling the authors of the work used not only the constant cooling rates, but temperature cycles based on modified Rozenthal equations [13] — analytical solutions for temperature fields during weld-

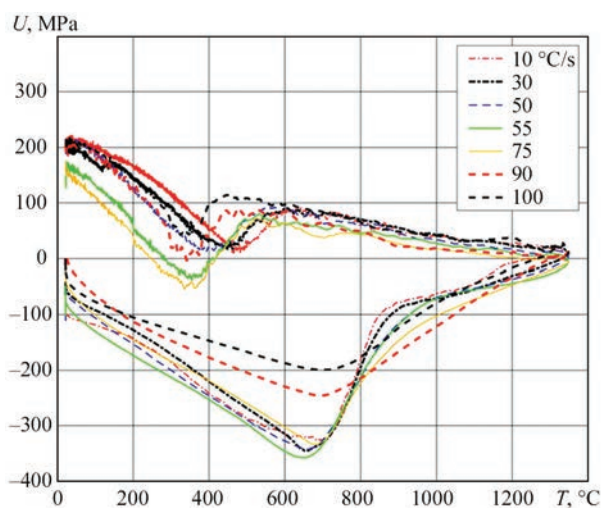


Figure 7. WTSD diagram for high-strength low-alloy steel [12] ing, allowing for the speed of heat source movement, material thermal conductivity and other parameters. During the experiment, the reactive forces, i.e. the force generated in response to the thermal expansion and compression of the sample, were recorded. These characteristics were used to determine the magnitudes of mechanical stresses (thermal and residual), plotted as the function of temperature. This allowed obtaining diagrams of σ – T type (stress — temperature) for each mode (Figure 7).

Result analysis revealed (Figure 7) that the maximal residual stresses do not always arise at the highest or lowest cooling rates, as is commonly believed. For examples, maximal stresses were recorded in the CGHAZ zone at a medium cooling rate of 50 °C/s. The reason for this is a complex interaction between the phase transformations (particularly, formation of martensite) and limitation of thermal expansion.

In the conclusions the authors state that WTSD is an efficient tool for assessment and simulation of re-

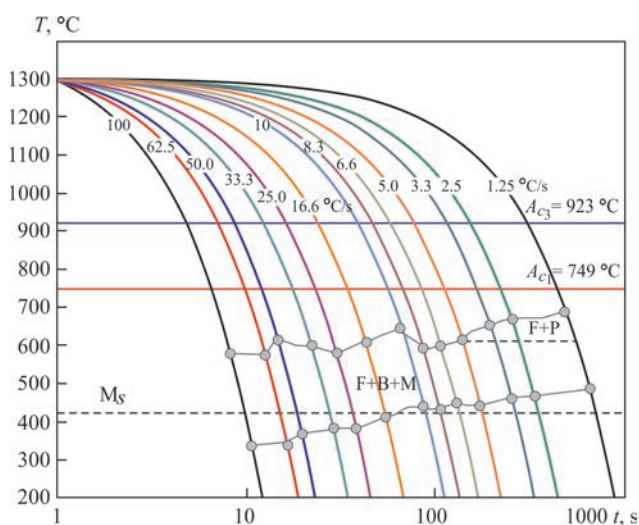


Figure 8. CCT diagram for 700MC steel. Microstructures: F — ferrite; B — bainite; P — pearlite; M — martensite; M_s — start of martensitic transformation [14]

sidual stresses in welded joints, particularly, when using modern steels sensitive to cracking. This method can be also used for calibration of numerical models of stresses and mechanical properties of the metal after welding.

Under the real conditions of the welding process, metal cooling occurs at a changing rate, which depends on the heat removal, joint geometry, welding mode and other factors. Linear modes do not reflect these peculiarities, so they do not allow adequate modeling of the structural transformations in the HAZ. Use of nonlinear cycles close to the real ones ensures higher reliability of the results, and allows a more accurate reproduction of the conditions of microstructure formation in the welded joint.

In [14] application of nonlinear thermal cycles for CCT diagram construction is substantiated by the inconsistencies and errors in the diagrams, plotted using constant cooling rates, and the desire to bring physical modeling closer to the real welding conditions. The work presents the results of physical modeling of the structure and phase transformations in the CGHAZ of structural steel 700MC (C — 0.065 %; Mn — 1.82 %; Al — 0.025 %; Cu — 0.0115 %; Cr — 0.025 %; Ni — 0.037 %; V — 0.014 %; Nb — 0.053 %; Ti — 0.102 %) (Figure 8).

Modeling was performed in Gleeble 3800 installation. Peak temperature of 1300 °C was selected for CGHAZ modeling, which corresponds to the temperature field near the weld. Heating rate was equal to 100 °C/s with soaking for 1 s at maximal temperature. 13 variants of cooling at the rate from 1.25 up to 100 °C/s were realized. The cooling cycles were nonlinear with application of Rykalin model [15]. This model also is an analytical scheme of heat transfer, which allows for temperature distribution in massive welded parts, taking into account the material geometry, heat conductivity and density. Its application is due to the need to accurately model the heterogeneous thermal conditions in thick-walled welded structures, where the linear models give significant errors. The authors came to the conclusion that accurate physical modeling of CGHAZ with application of nonlinear thermal cycles allows reliably plotting the CCT diagrams, specific exactly for welding. In particular, during optimization of the welding modes for 700MC steel the cooling rates above 25 °C/s should be avoided, so as to prevent excess martensite formation, which is accompanied by an increase in hardness and lowering of metal toughness in the HAZ.

The main objective [16] was to study the influence of the cooling mode on the structural-phase composition of the HAZ metal of 15Kh2NMFA steel, used in the bodies of WWER-1000 reactors in arc surfacing.

The authors tried to compare the theoretical concepts based on standard thermokinetic diagrams, with the real conditions of structure formation during welding/surfacing. As the real surfacing process is characterized by nonlinear cooling, which is considerably different from the linear cycles, both physical modeling maximum close to the welding/surfacing conditions, and a number of experiments using the linear cooling cycles were conducted. The authors sought to verify how the real conditions will influence the formation of the final microstructure. In order to plot the classical thermokinetic diagrams the samples of 15Kh2NMFA steel were heated to 1000 °C, held at this temperature for 170 min, and then cooled at different constant rates (1, 3, 5 and 7 °C/s).

When modeling cycles close to the real welding conditions, two series of experiments were conducted in which the samples were heated to 1000 or to 1350 °C. Then the samples were cooled at the rates of 3, 4 and 5 °C in the range of 800–500 °C for both the series. All the experimental work was conducted in Gleeble 3800.

A key difference of the real surfacing cycles from the linear ones (for plotting the CCT diagrams) is an extremely short time of the metal staying at the austenitization temperature (~ 1 s). During short holding and further cooling under the conditions close to the surfacing ones, the metal can form a totally martensitic structure, whereas during linear cooling at similar cooling rates a bainitic-martensitic structure is formed.

A change in the maximal heating temperature (1000 against 1350 °C) practically did not influence the kinetics of the martensite phase formation, and only slightly affected the temperatures of the start/finish of phase formation. However, this change influenced the maximal fraction of the phases in the final microstructure, which points to the importance of allowing for the peak cycle temperature.

The authors of the work convincingly showed that the cooling mode, in particular the nonlinearity and the extremely short time of staying at the austenitization temperature, is of a decisive importance for formation of the structural-phase composition in the HAZ of 15Kh2NMFA steel. Application of standard CCT diagrams constructed on the base of linear cooling cycles with a long holding time does not allow adequately predicting the microstructure under the conditions of the real welding process. For accurate prediction it is necessary to use experimentally plotted CCT diagrams, derived under the conditions maximum close to the actual thermal cycles of surfacing, allowing for the specifics of their nonlinearity and the short time of austenitization.

CONCLUSIONS

1. Continuous cooling transformation diagrams (CCT) are an important tool to predict the structure in the heat-affected zone of welded joints. Their construction is based on dilatometric experiments with a constant cooling rate. Such an approach, however, only partially corresponds to the real welding conditions.

2. The deformation continuous cooling transformation diagrams (DCCT) allow for the influence of plastic deformation, which can significantly change the phase transformation kinetics, in particular, accelerate formation of pearlite and bainite and lower the temperature of martensitic transformation.

3. Allowing for the complex temperature-mechanical effects (residual stresses, real temperature gradients, etc.) enables more accurately predicting the possible level of residual stresses, depending on the material cooling rate.

4. Nonlinear thermal cycles, which model the real cooling during welding, provide more accurate correspondence of the phase transformations with the actual welding conditions. Their application allows construction of more relevant diagrams, and avoiding the errors inherent in linear models.

5. Physical modeling in Gleeble installations remains the key method to investigate the thermal behaviour of steels in welding under the condition of correct setting up of the experiment, allowing for both the temperature and deformation parameters.

REFERENCES

1. Atkins, M. (1980) *Atlas of continuous cooling transformation diagrams for engineering steels*. Rev. U.S. Ed. Metals Park, Ohio, ASM International.
2. Seyffarth, P., Meyer, B., Scharff, A. (1992) *Großer atlas schweiß-ZTU-Schaubilder*. Düsseldorf, Deutscher Verlag für Schweißtechnik, DVS-Verl.
3. Zhang, Z., Farrar, R. A. (1995) *An atlas of continuous cooling transformation (CCT) diagrams applicable to low carbon low alloy weld metals*. London, The Institute of Materials.
4. Kostin, V.A., Zhukov, V.V. (2021) Improvement of the procedure of analysis of thermokinetic diagrams of phase transformations in metal of high-strength low-alloy steel welds. *Suchasna Elektrometalurhiya*, **2**, 40–46 [in Ukrainian]. DOI: <https://doi.org/10.37434/sem2021.02.06>
5. (2023) ASTM A1033-18: *Standard practice for quantitative measurement and reporting of hypoeutectoid carbon and low-alloy steel phase transformations*. ASTM International. DOI: <https://doi.org/10.1520/A1033-18R23>
6. Li, H., Liang, J.-L., Feng, Y.-L., Huo, D.-X. (2014) Microstructure transformation of X70 pipeline steel welding heat-affected zone. *Rare Metals*, **33**(4), 493–498. DOI: [10.1007/s12598-014-0344-x](https://doi.org/10.1007/s12598-014-0344-x)
7. Vimalan, G., Muthupandi, V., Ravichandran, G. (2018) Construction of continuous cooling transformation (CCT) diagram using gleeble for coarse grained heat affected zone of SA106 grade B steel. In: *Proc. of Conf. on AIP*, **1966**, 020013. DOI: <https://doi.org/10.1063/1.5038692>

8. Zheng, S., Wu, Q., Huang, Q., Liu, S., Han, Y. (2011) Influence of different cooling rates on the microstructure of the HAZ and welding CCT diagram of CLAM steel. *Fusion Eng. and Design*, **86**, 2616–2619. DOI: <https://doi.org/10.1016/j.fusengdes.2011.02.072>
9. Wu, Q.-s., Zheng, S.-h., Huang, Q.-y., Liu, S.-j., Han, Y.-y. (2013) Continuous cooling transformation behaviors of CLAM steel. *J. of Nuclear Materials*, **442**, S67–S70. DOI: <https://doi.org/10.1016/j.jnucmat.2013.03.072>
10. Kawulok, R., Schindler, I., Kawulok, P. et al. (2015) Effect of plastic deformation on CCT diagram of spring steel 51CrV4. In: *Proc. of Conf. on METAL 2015*, 345–350.
11. Ali, M., Kaijalainen, A., Hannula, J. et al. (2020) Influence of chromium content and prior deformation on the continuous cooling transformation diagram of low-carbon bainitic steels. *Key Eng. Materials*, **835**, 58–67. DOI: <https://doi.org/10.4028/www.scientific.net/KEM.835.58>
12. Mishchenko, A., Scotti, A. (2021) Welding thermal stress diagrams as a means of assessing material proneness to residual stress. *J. of Materials Science*, **56**, 1694–1712. DOI: <https://doi.org/10.1007/s10853-020-05294-y>
13. Rosenthal, D. (1946) The theory of moving sources of heat and its application to metal treatments. *Transact. of the American Society of Mechanical Eng.*, **68(8)**, 849–866. DOI: <https://doi.org/10.1115/1.4018624>
14. Roshan, R., Naik, A.K., Saxena, K.K., Msomi, V. (2022) Physical simulation on joining of 700MC steel: A HAZ and CCT curve study. *Materials Research Express*, **9(4)**, 046522. DOI: <https://doi.org/10.1088/2053-1591/ac6792>
15. Rykalin, N.N. (1960) Calculation of heat processes in welding. In: *42nd Annual Meeting of the American Welding Society*.
16. Lobanov, L.M., Kostin, V.A., Makhnenko, O.V. et al. (2020) Forecasting of structural transformations in HAZ steel of

15Kh2NMFA at anti-corrosion cladding. *Problems of Atomic Sci. and Technology*, **126(2)**, 89–96. DOI: <http://dx.doi.org/10.46813/2020-126-089>

ORCID

V.V. Zhukov: 0000-0002-3358-8491,
V.A. Kostin: 0000-0002-2677-4667,
S.G. Hrygorenko: 0000-0003-0625-7010,
R.S. Gubatyuk: 0000-0002-0851-743X

CONFLICT OF INTEREST

The Authors declare no conflict of interest

CORRESPONDING AUTHOR

V.V. Zhukov
E.O. Paton Electric Welding Institute of the NASU
11 Kazymyr Malevych Str., 03150, Kyiv, Ukraine.
E-mail: zhukov.kyiv@gmail.com

SUGGESTED CITATION

V.V. Zhukov, V.A. Kostin, S.G. Hrygorenko,
R.S. Gubatyuk (2025) Modern approaches
to obtaining continuous cooling transformation
diagrams for welding (Review).
The Paton Welding J., **10**, 16–23.
DOI: <https://doi.org/10.37434/tpwj2025.10.03>

JOURNAL HOME PAGE

<https://patonpublishinghouse.com/eng/journals/tpwj>

Received: 09.06.2025

Received in revised form: 08.08.2025

Accepted: 21.10.2025

